

# Metrics for multirate routing in dense LEO constellations

Jonas W. Rabjerg, Israel Leyva-Mayorga, and Beatriz Soret  
Department of Electronic Systems  
Aalborg University, 9220, Aalborg, Denmark  
Email: jrabje16@student.aau.dk, ilm@es.aau.dk, bsa@es.aau.dk

**Abstract**—Low Earth Orbit (LEO) satellite constellations combine great flexibility and global coverage with short propagation delays when compared to satellite networks deployed in higher orbits. However, the fast movement of the individual satellites makes inter-satellite routing a complex and dynamic problem. In this paper, we investigate the performance with three routing metrics in terms of routing latency. Besides, we provide the formulations to calculate the total latency considering the predictable propagation and packet transmission times in single- and multi-packet transmissions with different rates at the satellites. Our results showcase the contribution of each of these aspects to the total routing latency. In addition, these emphasize that the overall minimum latency can only be achieved by combining a metric that calculates the per-packet latency at each feasible hop with a path selection algorithm that considers the successive packet transmissions. Doing so leads to latency savings of up to 40% when compared to performing successive packet transmissions using Dijkstra’s shortest path algorithm at the expense of increasing the routing complexity. Nevertheless, closely similar results are achieved with one of the presented metrics, the path loss metric, in combination with Dijkstra’s algorithm. Besides, we observe that the impact of the queuing latency at the nodes greatly depends on the selected metric and the number of packets to be transmitted. These aspects can be used to design metrics and algorithms for specific types of services.

## I. INTRODUCTION

Low Earth Orbit (LEO) satellite constellations are usually organized in orbital planes. These are groups of satellites, deployed at altitudes from 600 to 2000 km above the Earth’s surface, that orbit in the same direction, one after the other. Fig. 1 shows an example of a typical Walker star constellation with five orbital planes and 200 satellites deployed at an altitude of  $\approx 1000$  km. These satellites communicate with ground stations (GS) or user equipment on the Earth surface through the ground-to-satellite link (GSL). On the other hand, communication between satellites may take place through the inter-satellite link (ISL), which are not always implemented, mainly due to cost and physical constraints in the satellites [1]. Nevertheless, implementing the ISLs in a constellation is essential for systems that aim at serving as a space backbone network for latency-sensitive services without depending on geo-stationary satellites or a dense network of GSs.

As illustrated in Fig. 1, the ISLs can be further divided into intra- and inter-plane ISLs. Intra-plane ISLs communicate neighboring satellites in the same orbital planes, using antennas located at both sides of the roll axis. Since the

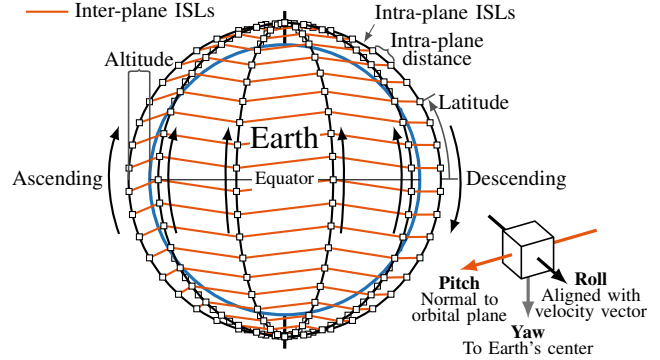


Fig. 1: Diagram of a Walker star constellation with five orbital planes and the axes of a satellite with respect to the velocity vector. Arrows near the orbital planes indicate the direction of rotation.

inter-satellite distances within the same orbital planes are mainly fixed, intra-plane ISLs are usually stable and ultra-narrow beams, for example, optical wireless links, can be used [2]. On the other hand, satellites in different orbital planes communicate through the inter-plane ISLs, using antennas located at both sides of the pitch axis. Note that the rapid movement of the satellites creates frequent changes in the relative positions between satellites in different orbital planes. Therefore, inter-plane ISLs are greatly dynamic and may be affected by Doppler shift. Nevertheless, both intra- and inter-plane ISLs are needed to ensure full connectivity across the constellation and to enable the interconnection of ground devices across the globe from the space.

In order to have routing capabilities in the constellation, ISLs must be implemented together with a routing protocol, which is responsible of finding appropriate routes between any two satellites according to the selected routing metric and of defining the forwarding rules. Routing metrics are an essential element of routing protocols, which are used to determine the cost of each potential hop towards the destination. Classical examples of routing metrics in terrestrial networks include the number of hops (i.e., hop-count), the expected number of transmissions due to packet erasures, euclidean distance, etc. In traditional unipath routing, these metrics are used to identify and select the path with the lowest total cost before the packet is actually transmitted from the source. On the other

hand, in opportunistic routing, routes are dynamic rather than fixed. This aims to exploit the broadcast nature of the wireless channel in the presence of transmission failures [3].

Routing for LEO satellite constellations has been investigated for years. The first set of relevant works for this paper are from the times of the initial Iridium launches. For example, Ekici *et al.* [4] proposed a routing approach that exploits the geometry of a symmetric Walker star constellation. Intervals in the latitude of the satellites, known as *logical locations* were defined. Then, to route the packets, rings were formed with satellites from different orbital planes that are at the same logical locations. However, this approach is not efficient for constellations with slight asymmetries, as pointed out in our previous work [5]. These slight asymmetries can be found in most commercial dense LEO constellations, in the form of slightly different altitudes at the orbital planes, to minimize the risk of collisions between satellites. Hence, with the advent of the New Space era, there is a renewed interest in satellite routing [6], [7].

To the best of our knowledge, the efforts in previous works have oversimplified the constellation geometry and the ISL connectivity, with the exception of papers studying specific commercial constellations such as [7]. In a general approach, we observe that the characteristics of the constellation introduce two distinctive elements to the routing problem. First of all, the constellation geometry represents a structured dynamic wireless mesh network, where the distances between satellites: 1) in the same orbital plane are fixed and 2) in different orbital planes change rapidly. Secondly, the propagation time has a great impact in the overall latency. This is in contrast to terrestrial wireless mesh networks, where the propagation time is negligible when compared to the transmission time (i.e., time to transmit  $b$  bits at a given data rate). This aspect requires special attention in the design of routing protocols for LEO constellations.

Under these premises, we investigate routing metrics relevant for LEO satellite constellations supporting latency-sensitive services. Our analyses exploit the predictability component of the latency, namely the propagation and the transmission latency, in the routing. To this end, we consider an exemplary network where two ground users, separated by a great distance, communicate with each other through the constellation. For this, the ground users communicate, either directly or through a dedicated GS, with the nearest LEO satellite. In this scenario, we investigate three different routing metrics and assess the performance using unipath routing with multiple rates (i.e., multirate routing) in the dense Walker star LEO constellation illustrated in Fig. 1.

The rest of the paper is organized as follows. Section II presents the system model, followed by the detailed description of the routing metrics in Section III. Then, Section IV presents our results and Section V concludes the paper.

## II. SYSTEM MODEL

In this section, we present the constellation geometry and the channel model used for our analyses. While the LEO

constellation is dynamic, we observe the entire system at specific time instants  $t \in \mathbb{R}^+$  and skip the time dependence  $t$  for notation simplicity throughout this section.

We consider a Walker star constellation, as in [5], with  $M$  polar planes evenly separated by  $\pi/M$ . An orbital plane  $a \in \{1, 2, \dots, M\}$  consists of  $N_a$  evenly spaced satellites deployed at an altitude  $h_a$  and with an inclination angle  $\epsilon_a = (a - 1)\pi/M$ . The latitude of each satellite, measured from the Equator towards the north pole as in Fig. 1, is denoted as  $\theta_i$ , where  $a$  is the orbital plane and  $i' \in \{1, 2, \dots, N_a\}$  is the index of satellite  $i$  within the orbital plane. Building on these, the coordinates of satellite  $i$  in an orbital plane  $a$  are given as  $(h_a + r_E, \epsilon_a, \theta_i)$ , where  $r_E$  is the radius of the Earth.

We model the satellite constellation as a weighted undirected graph  $G = (V, E)$ , where  $V$  is the set of satellites (i.e., vertices) and  $E$  is the set of edges (i.e., ISLs). The satellites are equipped with four antennas for inter-satellite communication: two antennas for the intra-plane ISLs – aligned and opposite to the roll axis, in the direction of the velocity vector – and two for the inter-plane ISLs – one at each side of the pitch axis, normal to the orbital plane (see Fig. 1). Building on this, satellites maintain a connection with their closest inter- and intra-plane neighbors, one at each side of the pitch and roll axes, at all times as illustrated in Fig. 1. These connections constitute the set of edges  $E$  of the network graph.

The weights  $w(e)$  for all  $e \in E$  are defined in the following section for the selected routing metrics. Therefore, the route of a single packet is a weighted path  $P$  in  $G = (V, E)$  with edge set  $E(P)$ . Note that we do not account for the latency on the ground-to-satellite and satellite-to-ground links. This is because, given that the source and destination satellites – the ones closest to the source and destination GSs – are the same for all possible paths, these links would simply add a constant latency to the results presented in Section IV.

Inter-satellite communication occurs in a free-space path loss (FSPL) environment. Let  $l(i, j)$  be the slant range (i.e., line-of-sight distance) between two arbitrary satellites,  $i$  and  $j$ , calculated as the euclidean norm between their positions. Next, let  $L_p(i, j)$  be the FSPL and  $f$  be the carrier frequency. All the antennas have fixed transmission power  $P_t$  and gains in the direction of the main lobe, denoted as  $G_t$  for transmission and  $G_r$  for reception. Hence, the received signal strength at  $j$  from  $i$  is

$$P_r(i, j) = \frac{P_t G_t G_r}{L_p(i, j)} = P_t G_t G_r \left( \frac{4\pi l(i, j) f}{c} \right)^{-2}, \quad (1)$$

where  $c$  is the speed of light [8].

We consider typical parabolic reflector antennas with perfect beam steering capabilities [9], whose gain with respect to a perfect isotropic antenna is the function of the diameter of the reflecting surface  $D$ , the carrier frequency  $f$ , and the efficiency of the antenna  $k$ , given as

$$G_t = G_r = k \left( \frac{\pi D f}{c} \right)^2. \quad (2)$$

From (2), it can be seen that using a high carrier frequency will result in a higher antenna gain if the same parabolic reflector is being used.

It is out of the scope of this paper to design or evaluate interference mitigation techniques and we assume the interference to an ongoing transmission is zero at all times. This can be achieved either by using sufficiently narrow beams or by diverse multiple access techniques that assign orthogonal resources for communication such as TDMA, FDMA, OFDMA, or even CDMA with a sufficiently large spreading factor.

Based on this latter assumption, we consider that intersatellite communication takes place in an additive white Gaussian noise (AWGN) channel. Hence, we deal with a multirate routing problem where, for simplicity, the data rate for communication between  $i$  and  $j$  is selected for a known received power  $P_r(i, j)$ , from an infinite set of possible values, to be

$$\begin{aligned} R(i, j) &= B \log_2 \left( 1 + \frac{\text{SNR}(i, j)}{\gamma} \right), \\ &= B \log_2 \left( 1 + \frac{P_r(i, j)}{k_B T_s B \gamma} \right), \end{aligned} \quad (3)$$

where  $B$  is the bandwidth,  $k_B$  is Boltzmann's constant,  $T_s$  is the system noise temperature, and  $\gamma$  is the SNR margin selected to transmission failures in the presence of interference. Note that our analyses can be easily extended to the case where the rates are selected from a finite set of feasible values.

Knowing the data rate for communication between  $i$  and  $j$  and the state of the queues at the satellites, the exact one-hop latency to transmit a packet of length  $p$  bits can be calculated in three parts. First, the time it takes for the electromagnetic radiation to travel the distance  $l(i, j)$  from  $i$  to  $j$ , which we refer to as the *propagation time*. Second, the time it takes to transmit  $p$  bits at  $R(i, j)$  bps, which we will refer to as the *transmission time*. Finally, the *waiting time* at the queue  $t_w(i, j)$ , which is an observation of the random variable (RV)  $T_w(i, j)$ . Hence, we have

$$\text{Latency}(i, j) = \underbrace{\frac{l(i, j)}{c}}_{\text{Propagation time}} + \underbrace{\frac{p}{R(i, j)}}_{\text{Transmission time}} + \underbrace{t_w(i, j)}_{\text{Waiting time}}. \quad (4)$$

Next, considering that the propagation, transmission, and waiting times are negligibly short when compared to the movement of the constellation, the overall latency when successively transmitting  $n$  packets of the same size  $p$  through the same path  $P$  can be calculated as

$$\begin{aligned} \text{Latency}(P, n) &\approx (n-1) \max_{e \in E(P)} \left\{ \frac{p}{R(e)} \right\} + \sum_{e \in E(P)} \frac{l(e)}{c} + \frac{p}{R(e)} + t_w(e) \\ &\leq \sum_{e \in E(P)} \frac{l(e)}{c} + \frac{np}{R(e)} + t_w(e). \end{aligned} \quad (5)$$

Note that (5) is an approximation due to the fast movement of the satellites, which creates minor changes in the latency, even

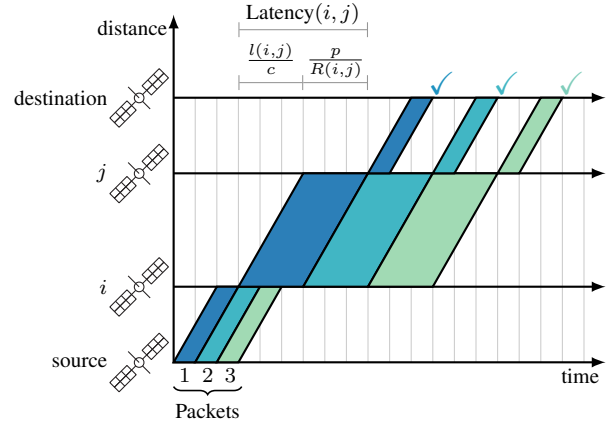


Fig. 2: Time diagram for the transmission of three packets along a three-hop route. Satellites are at different distances and use different transmission rates.

between short time instants. Nevertheless, (5) indicates that, even if no transmission errors occur, successively transmitting  $n > 1$  packets of  $p$  bits each is more efficient than transmitting a *big* packet of size  $np$ . On the other hand, the last term in (5) is a tight upper bound as  $\text{Latency}(P, p, 1) = \sum_{e \in E(P)} l(e)/c + p/R(e) + t_w(e)$ . These characteristics are illustrated in Fig. 2, where three packets are transmitted along a same path with three hops with zero waiting time at the queues. Note that the ISL between  $i$  and  $j$  has the greatest transmission time and, hence, the greatest contribution to the overall latency.

However, knowing the status of the queues at all satellites is a daunting task with great communication overhead. For instance, all satellites would need to report the status of their queues to the nodes calculating the routes ahead of time. Instead, routing metrics usually focus on finding the shortest path for each packet considering zero queueing delay at each hop, as illustrated in Fig. 2. Nevertheless, this completely neglects the waiting time at the queues. A feasible alternative to incorporate these waiting times is to calculate a long-term average for  $T_w(e)$  across the constellation  $\mu_{T_w}$  and use it for routing purposes. By doing so, and assuming  $T_w(e) \sim \text{Exp}(1/\mu_{T_w})$  are i.i.d. RVs, the expected latency for 1) an ISL  $(i, j)$ , denoted  $\mu_{\text{Latency}}(i, j)$ , and for 2) a path  $P$ , denoted  $\mu_{\text{Latency}}(P, n)$ , can be calculated by substituting  $t_w(e)$  with  $\mu_{T_w}$  in (4) and (5), respectively.

### III. ROUTING METRICS

In this section we describe in detail the three considered routing metrics.

**Hop-count metric:** This is one of the simplest routing metrics, where the cost (i.e., weight) of every hop is set to the same value, for example,  $w(i, j) = 1$  for all  $i$  and  $j$ . If two or more paths have the same cost, the one with the shortest transmission distance is selected. Due to its simplicity, we use this metric as a benchmark.

**Latency:** The aim of the latency metric is to deliver the packets using the minimal amount of time. For this, the

weight of all edges is  $w(i, j) = \mu_{\text{Latency}}(i, j)$ , so that both the propagation and transmission times are considered, along with the mean waiting time at the queue.

The main benefit of the latency metric is that it accounts for 1) the linearity of the propagation times, 2) the non-linearity of the path loss and, hence, of the achievable data rate  $R(i, j)$  as defined in (3), and 3) the mean waiting time at the queues. Note that a simpler version of this metric can be obtained by setting  $\mu_{T_w} = 0$ , which is beneficial when the waiting times are not adequately characterized by the latter parameter.

**Path loss metric:** This is a relatively simple metric that emphasizes the non-linearity of the path loss in the ISLs. Besides, it can be easily adapted to exploit the specific geometry of the considered constellation.

Let  $i$  be a satellite in orbital plane  $a$  and in a feasible routing path  $P$  towards the destination, located in orbital plane  $d$ . It is immediate to see that the overall latency is reduced by using the intra-plane ISL if  $a = d$ . Hence, we define  $\mathbb{1}_{a \neq d}$  to be an indicator variable that takes the value of 1 if  $a \neq d$  and 0 otherwise. Then, we set the cost of all intra-plane ISLs to be  $w_{\text{intra}}(i, j) = 1$ .

On the other hand, the cost of the inter-plane ISLs towards the closest neighbor  $j$  in orbital plane  $b$  is set to be the ratio of inter- to intra-plane path loss, given as

$$\begin{aligned} w_{\text{inter}}(i, j) &= \frac{L_p^{\text{inter}}(i, j)}{L_p^{\text{intra}}(i, j')} \\ &= \left[ (h_a + r_E)^2 + (h_b + r_E)^2 - 2(h_a + r_E)(h_b + r_E) \right. \\ &\quad \times \left. \left( \sin \theta_i \sin \theta_j + \cos \frac{\pi}{M} \cos \theta_i \cos \theta_j \right) \right] \\ &\quad \times \left( \mathbb{1}_{a \neq d} \left( 4(h_a + r_E)^2 \sin^2 \frac{\pi}{N_a} \right) \right)^{-1}, \end{aligned} \quad (6)$$

where  $j'$  is the closest intra-plane neighbor of  $i$ . Note that  $j$  is the closest inter-plane neighbor to  $i$  in  $b$  if and only if  $\theta_j \in [\theta_i - 2\pi/N_b, \theta_i + 2\pi/N_b]$ .

Therefore, (6) can be closely approximated by assuming that all orbital planes are deployed at the same altitude  $h_a$  and that the satellites are aligned, so that  $\theta_i = \theta_j$ , as

$$w_{\text{inter}}(i, j) \approx \frac{\cos^2 \theta_i \left( 1 - \cos \left( \frac{\pi}{M} \right) \right)}{\mathbb{1}_{a \neq d} \left( 1 - \cos \left( \frac{2\pi}{N_a} \right) \right)}. \quad (7)$$

Naturally,  $w_{\text{inter}}(i, j)$  greatly depends on  $\theta_i$ , but also on the ratio  $M/N_a$ . Therefore, inter-plane ISLs are preferred when the packet is close to the poles, where  $\cos^2 \theta_i \approx 0$ , but also when  $M > N_a$ .

To illustrate the calculation of the path loss routing metric, we show the CDF of the FSPL to the nearest inter-plane neighbor as a function of the latitude of a given satellite  $i$ , denoted  $\theta_i$  (given in degrees), in Fig. 3. These were obtained via Monte Carlo simulations, considering the Walker star constellation illustrated in Fig. 1 with  $M = 5$ ,  $N_a = 40$ , and  $h_a = 1000 + 10(a - 1)$  km. The minimum and maximum FSPL to the nearest neighbor in the same orbital plane (i.e.,

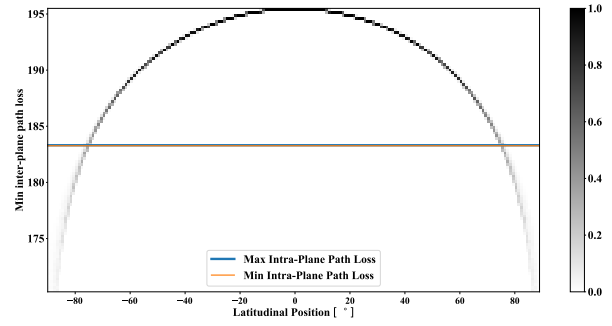


Fig. 3: Heatmap of the empirical probability mass function (pmf) of the FSPL to the nearest inter-plane neighbor, along with the maximum and minimum FSPL for the nearest intra-plane neighbor.

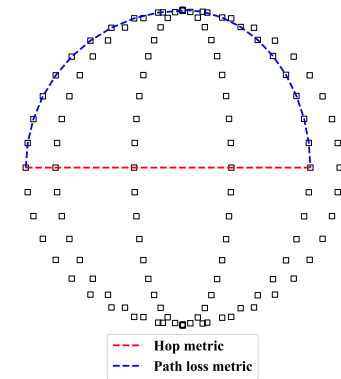


Fig. 4: Illustrative example of the paths selected by the hop-count and path loss metrics for GSs along the Equator and separated by an angle of  $\epsilon_{s,d} = 4\pi/5$ .

at the lowest and highest orbital planes, respectively) are also illustrated.

As Fig. 3 shows,  $L_p^{\text{inter}}(i, j) > L_p^{\text{intra}}$  for all  $|\theta| < 75^\circ$ . This illustrates the reason to calculate  $w_{\text{inter}}(i, j)$  as in (6). Specifically, the curvature of the heatmap represents the pmf of the numerator in (6), while the maximum and minimum intra-plane path loss, which are closely similar, represent the range of possible values for the denominator. The intersection describes when  $\theta_i$  is large enough to make the  $w_{\text{inter}}(i, j) = 1$ .

Based on these metrics, we find the shortest path using two approaches when a given number of successive packets  $n$  are transmitted. First, with Dijkstra's algorithm [10], which finds in the shortest path between source and destination considering a single packet transmission. This approach is used with all three metrics and leads to the minimum expected latency when combined with the latency metric for  $n = 1$ . Second, via exhaustive search (ES) in combination with the latency metric. That is, finding all the feasible paths in the constellation and the latency at each of the ISLs involved and, next, calculating the overall latency with (5) to find the shortest path. This leads to the minimum expected latency for any  $n \in \mathbb{N}^+$ .

Fig. 4 shows an illustrative example of the difference

TABLE I: Simulation parameters

Parameter	Symbol	Value
# of orbital planes	$M$	5
# of satellites per orbital plane	$N_a$	40
Height of plane $a$	$h_a$	$1000 + 10(a - 1)$ km
Separation between GSs	$\epsilon_{s,d}$	$\{4\pi/5, \pi/5\}$ rads
Packet size	$p$	1470 bytes
# of packets	$n$	$\{1, 20\}$
Transmission power	$P_t$	10 W
Parabolic reflector diameter	$D$	0.1 m
Parabolic antenna efficiency	$k$	0.5
System temperature	$T_s$	1500 K
SNR margin (see (3))	$\gamma$	2 dB
<b>Setup I</b>		
Carrier frequency	$f$	30 GHz
Bandwidth	$B$	1.5 GHz
Antenna gains (from (2))	$G_t, G_r$	26.94 dB
<b>Setup II</b>		
Carrier frequency	$f$	12 GHz
Bandwidth	$B$	0.65 GHz
Antenna gains (from (2))	$G_t, G_r$	18.98 dB
Mean transmission time in the intra-plane ISLs	$\mu_{\text{intra}}$	1.464 ms
Mean length of the queues	$\mu_Q$	$\{0, 2\}$

between the routes selected with the hop-count and the path loss metrics in a scenario where the source and destination satellites are located along the equator, separated by an angle of  $\epsilon_{s,d} = 4\pi/5$ . Note that this is the worst case routing scenario, since the longest distances for inter-plane ISLs and the highest number of intra-plane hops toward the poles occur along the Equator. Hence, this is one of the selected scenarios to evaluate the performance of the routing metrics in the following section.

Throughout our analyses, we express the mean waiting time at the queues  $\mu_{T_w}$  as a function of the expected transmission time for one packet through the intra-plane ISLs  $\mu_{\text{intra}}$ . From there, we define  $\mu_{T_w} = \mu_Q \mu_{\text{intra}}$  where  $\mu_Q$  represents the mean length of the queue.

#### IV. RESULTS

In this section, we present the performance analysis of the three routing metrics in two setups for  $n \in \{1, 20\}$ . In each setup, we consider the use of different carrier frequencies  $f$  and bandwidths  $B$ . As it will be seen, the contribution of the propagation and transmission times in each of these setups is different. Besides, for Setup I, we consider two values for the separation between source and destination  $\epsilon_{s,d} \in \{2\pi/5, 4\pi/5\}$ , and set  $\mu_Q = 0$  so the average waiting times in the queues  $\mu_{T_w} = 0$ . This choice of  $\mu_Q = 0$  represents a network with negligibly low load or the transmission of high priority packets following a preemptive approach. For Setup II, we set  $\epsilon_{s,d} = 4\pi/5$  and  $\mu_Q \in \{0, 2\}$ . The rest of the simulation parameters, selected from [5] and [9], are listed in Table I.

Simulation scripts to obtain the results have been developed in Python 3.7.6. At least 1000 simulations were run to obtain the mean values and empirical distribution functions presented in this section. In each simulation,  $n$  packets are transmitted successively as illustrated in Fig. 2 according to the selected

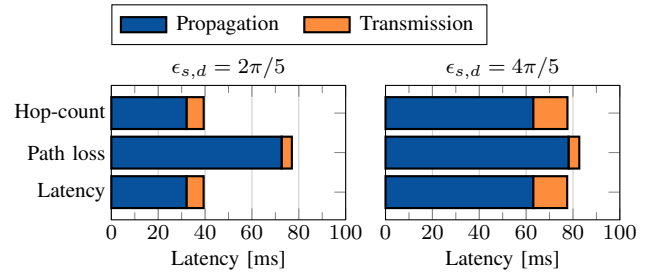


Fig. 5: Contribution of the propagation and transmission times to the expected routing latency with Setup I for  $n = 1$  and  $\epsilon_{s,d} = \{2\pi/5, 4\pi/5\}$ .

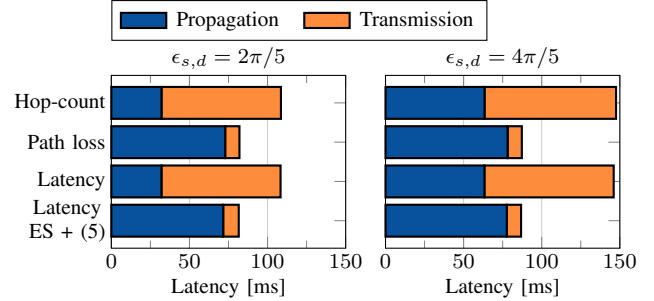


Fig. 6: Contribution of the propagation and transmission times to the expected routing latency with Setup I for  $n = 20$  and  $\epsilon_{s,d} = \{2\pi/5, 4\pi/5\}$ .

metric and shortest path algorithm. Namely, Dijkstra's algorithm for the three considered metrics, along with the latency metric with ES combined with (5) to find the shortest path with  $n > 1$ . The latter leads to the minimum possible latency. The period between simulations is set to be 20000 seconds, which allows for the satellites complete up to 4 rotations around the Earth to generate distinct routing scenarios.

**Setup I:** Due to the high carrier frequency and bandwidth, this setup leads to high data rates. Hence, propagation times have a greater impact on the overall latency than transmission times in this setup. This can be observed in Fig. 5, where the hop-count and latency metrics result in a shorter latency than the path loss metric for  $n = 1$  and both values of  $\epsilon_{s,d}$ . This is mainly because the path loss metric favours long paths with short transmission times at each hop. This increases the propagation time, which has a great contribution to the overall latency in this setup.

Next, Fig. 6 shows the routing latency for  $n = 20$ . In this case, the path loss metric leads to up to a 40% lower routing latency than the hop-count and latency metrics, and is up to the par with the overall minimum. This is because the path loss metric exploits the use of high data rates and, hence, short transmission times, which have a great impact on (5). Conversely, the latency metric with Dijkstra's algorithm fails to do so since it does not account for the exact total latency, described by (5), where the hop with the lowest data rate has an important contribution.

**Setup II:** This setup leads to lower data rates and, hence,



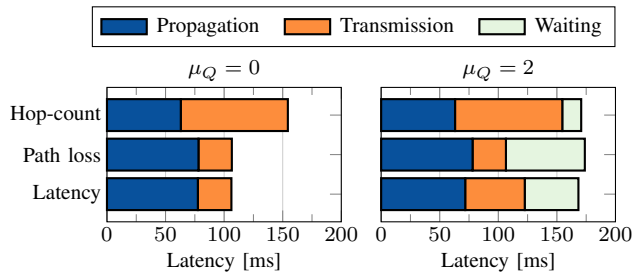


Fig. 7: Contribution of the propagation, transmission, and waiting times to the expected routing latency with Setup II for  $\mu_Q \in \{0, 2\}$ ,  $n = 1$ , and  $\epsilon_{s,d} = 4\pi/5$ .

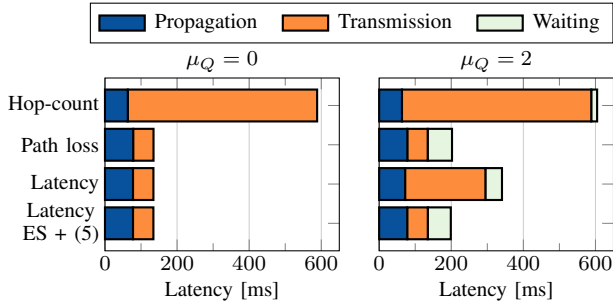


Fig. 8: Contribution of the propagation, transmission, and waiting times to the expected routing latency with Setup II for  $\mu_Q \in \{0, 2\}$ ,  $n = 20$ , and  $\epsilon_{s,d} = 4\pi/5$ .

longer transmission times than Setup I. Hence, we use it to illustrate the potential impact of waiting times at the queues. For this, Fig. 7 shows the contribution of propagation, transmission, and waiting times to the overall latency when transmitting a single packet. It is interesting to observe that a closely similar latency is achieved with the path loss routing and latency routing metrics with  $\mu_Q = 0$ . On the other hand, the propagation, transmission, and waiting times are widely different with the three metrics for  $\mu_Q = 2$ . Among these, the paths selected with the path loss metric are the most affected by queueing times.

Next, Fig. 8 shows the average routing latency for  $n = 20$ . Here, we again observe that the path loss metric performs up to the par with the optimal solution provided by the latency metric with ES and (5). Conversely, the latency metric with Dijkstra’s algorithm fails to do so with  $\mu_Q = 2$ . Besides, in contrast with Fig. 7, the contribution of the waiting times to the overall latency is much smaller than that of the transmission times. This is due to a greater ratio of transmission to waiting times with  $n = 20$  than with  $n = 1$ .

## V. CONCLUSION

In this article, we evaluated the efficiency of three routing metrics in a dense LEO constellation where the satellites can communicate at different data rates. In particular, we used Dijkstra’s algorithm to calculate the shortest path and considered the transmission of both a single and multiple packets successively. In addition, we provided the elements to

find the optimal path considering propagation, transmission, and mean waiting time at the queues through exhaustive search.

Our results show that, the latency metric – in which the weight of the ISLs is the expected latency – can be combined with Dijkstra’s algorithm to consistently find the optimal path when a single packet is transmitted. In contrast, combining the latency metric with Dijkstra’s algorithm to find the shortest path when successive packets are transmitted may lead to an excessive routing latency. Instead, the latency for successive packet transmissions can be reduced up to 40% with the use of the introduced path loss metric in combination with Dijkstra’s algorithm when compared to the latency metric. The reason for this is that this metric avoids long one-hop transmission times, which greatly contribute to the overall latency. In fact, the benefits of the path loss routing metric grow with the number of packets. This makes the path loss routing metric, in combination with the partitioning of the data into small packets, an appealing option for the transmission of broadband data.

As we have observed, there is the need for a novel shortest path algorithm that captures the effects of multiple rates and of successive packet transmissions from the same traffic flow in the queues of the satellites. Such algorithm, in combination with the latency metric, would lead to the selection of the (theoretically) shortest path as a function of the rates and the number of packets as described by (5).

## REFERENCES

- [1] I. del Portillo, B. Cameron, and E. Crawley, “A technical comparison of three low earth orbit satellite constellation systems to provide global broadband,” *Acta Astronautica*, vol. 159, 03 2019.
- [2] M. Motzigemba, H. Zech, and P. Biller, “Optical inter satellite links for broadband networks,” in *Proc. 9th International Conference on Recent Advances in Space Technologies (RAST)*, 2019, pp. 509–512.
- [3] A. Boukerche and A. Darehshoorzadeh, “Opportunistic routing in wireless networks: Models, algorithms, and classifications,” *ACM Computing Surveys*, vol. 47, no. 2, pp. 1–36, Nov. 2014.
- [4] E. Ekici, I. Akyildiz, and M. Bender, “A distributed routing algorithm for datagram traffic in LEO satellite networks,” *IEEE/ACM Transactions on Networking*, vol. 9, no. 2, pp. 137–147, Apr. 2001.
- [5] B. Soret, I. Leyva-Mayorga, and P. Popovski, “Inter-plane satellite matching in dense LEO constellations,” in *Proc. IEEE Global Communications Conference (GLOBECOM)*, 2019.
- [6] C. Han, L. Huo, X. Tong, H. Wang, and X. Liu, “Spatial anti-jamming scheme for Internet of Satellites based on the deep reinforcement learning and Stackelberg game,” *IEEE Transactions on Vehicular Technology*, vol. 9545, 2020.
- [7] M. Handley, “Delay is not an option: Low latency routing in space,” in *Proc. 17th ACM Workshop on Hot Topics in Networks*, nov 2018, pp. 85–91.
- [8] D. Tse and P. Viswanath, *Fundamentals of Wireless Communication*. Cambridge University Press, 2005.
- [9] I. F. Akyildiz and A. Kak, “The internet of space things/cubesats,” *IEEE Network*, vol. 33, no. 5, pp. 212–218, 2019.
- [10] N. Jasika, N. Alispahic, A. Elma, K. Ilvana, L. Elma, and N. Nosovic, “Dijkstra’s shortest path algorithm serial and parallel execution performance analysis,” in *Proc. 35th International Convention MIPRO*, 2012, pp. 1811–1815.